Interfacial Structure and Properties in Polystyrene/Epoxy Bilayer Films

H. S. JEON,[1] P. S. DIXIT,[1] H. YIM,[2] M. S. KENT,[2] K. SHIN,[3]* S. SATIJA[3]

[1] Department of Petroleum and Chemical Engineering, New Mexico Institute of Mining and Technology, Socorro, New Mexico

[2] Department 1811, Sandia National Laboratories, Albuquerque, New Mexico

[3] Reactor Division, National Institute of Standards and Technology, Gaithersburg, Maryland

Received 4 March 2002; revised 3 September 2002; accepted 12 September 2002

ABSTRACT: The interfacial structure and properties of immiscible deuterated polystyrene (*d*PS)/epoxy bilayer films were investigated with neutron reflectivity as functions of the composition of the epoxy layer, the thickness of the *d*PS layer, and the annealing time. We have found that the interfacial width and its growth rate depend strongly on the compositions of the epoxy layer but only weakly on the thickness of the *d*PS layer. The effect of the resin/crosslinker composition on the interfacial width and its growth rate is likely due to the different near-surface structures that result for different epoxy stoichiometries. For an ultra-thin *d*PS film (thickness = $2R_g$), the data suggest a slight suppression of the growth of the interfacial width that could be due to confinement effects for the long-chain molecules such as have been previously reported for a thickness of less than approximately $4R_g$, where R_g is the radius of gyration of polymer molecules. © 2002 Wiley Periodicals, Inc. J Polym Sci Part B: Polym Phys 40: 2653–2660, 2002
Keywords: crosslinking; interdiffusion; interfaces; neutron reflectivity; epoxy

INTRODUCTION

The interfacial structure and properties of thin polymer/polymer bilayer films are of great importance for practical applications as well as fundamental studies. In particular, the interfacial properties of asymmetric bilayer films play critical roles for various practical applications such as adhesion, protective coatings, and multilayer paints. The asymmetry can involve both chemistry and structure. Because most polymers are immiscible with each other, phase segregation between components is observed. The interfacial structure and properties largely determine the ultimate properties, and various theoretical approaches have been developed to predict the interfacial width and structure.[1–5] Recently, there have been many experimental studies of the structures of interfaces between thermoplastic polymers with neutron reflectivity (NR).[6–12] In particular, the interfacial width in bilayers of polystyrene (PS)/poly(methyl methacrylate) (PMMA) has been studied extensively with NR. The authors reported interfacial widths ranging from 40 to 70 Å, which depended on the PMMA (or PS) molecular weight and film thickness.[6–9] Merfeld et al.[11] used NR to study polyphenylene oxide (PPO)/styrene–acrylonitrile copolymer interfaces and found interfacial widths decreasing from approximately 65 to 10 Å as the copolymer composition increased from 15 to 40 wt % acrylonitrile.

Present address: *K-JIST, Kwangju, Korea
Correspondence to: H. S. Jeon (E-mail: jeon@nmt.edu)

Journal of Polymer Science: Part B: Polymer Physics, Vol. 40, 2653–2660 (2002)
© 2002 Wiley Periodicals, Inc.

Lin et al.[12] studied the rate of interdiffusion between deuterated and hydrogenated PMMA with NR and reported interfacial widths ranging from approximately 90 to 300 Å, which depended on the thickness of the deuterated PMMA layer. Despite the technical importance of thermoplastic/thermosetting interfaces, such as for protective coatings needed for improved mechanical and chemical properties, there are very few experimental studies of the interface structure of thermoplastic and highly crosslinked thermosetting systems. Bhala and Freakley[13] demonstrated that a nitrile–butadiene rubber coating applied as an antiozonent for the surface of a natural rubber substrate under static conditions can be effectively used as a protective coating. Wu et al.[14] reported a study of the diffusion of linear PS into a partially crosslinked PS network by NR and forward recoil scattering. They demonstrated that most of the linear chains diffused into the crosslinked network up to 200–300 Å when the molecular weight of the linear chain was comparable to or slightly greater than the molecular weight between crosslinks. In contrast, only a small amount of interdiffusion occurred when the molecular weight of the linear chain was much larger than the molecular weight between crosslinks. Kerle et al.[15,16] studied the interdiffusion of free chains into a chemically similar crosslinked matrix, with bilayers of a deuterated and hydrogenated copolymer of ethylene and butene-1. They reported that the extent of interdiffusion was proportional to the degree of crosslinking density of the network, and they observed a crossover from complete to partial wetting, followed by a second crossover back to complete wetting as the degree of crosslinking increased. The first transition was attributed to entropy-induced autophobicity, whereas the second transition was attributed to surface roughening.

In previous work, members of our group examined the structure of single-layer epoxy films on silicon substrates as a function of the composition and cure temperature with NR.[17] To study variations in the crosslink density, the samples were swelled with a good solvent, deuterated nitrobenzene. A variation in the crosslink density normal to the interface was inferred from the concentration profile of the solvent. The main result was a large degree of swelling near the air surface, indicating a lower crosslink density than in the bulk of the film. Also, greater equilibrium swelling and faster swelling kinetics were observed for the films deficient in curing agent relative to the films with an excess of curing agent, indicating a higher crosslink density in the latter case. We expect that the difference in the crosslink density at the surface may affect the interfacial width and its growth rate when a second film is applied on top of the epoxy film. Recently, the interfacial structure of thin epoxy/epoxy bilayer films before and after curing was also examined with NR.[18] The uncured components of the top layers were spun onto fully cured bottom layers, and then the top layers were cured. The principal observation was that an additional penetration of the components of the top layer into the bottom layer occurred upon curing. This additional penetration was dependent on both the molecular weight of the top layer and the cure temperature of the top layer relative to the glass-transition temperature of the bottom layer. Somewhat surprisingly, no variation in the interfacial width with the composition of the initial layer was observed.

In this study, we investigate the interfacial structure of bilayers of deuterated polystyrene (*d*PS) and a highly crosslinked thermosetting epoxy with NR. In these experiments, we have measured the interfacial width and surface roughness as functions of the thickness of the *d*PS layer, the composition of the epoxy layer, and the annealing time. The factors that control the interface width are not immediately obvious for thermoplastic/thermosetting systems. Although translational entropy drives intermixing, the degree of interpenetration may be limited either by the unfavorable enthalpic interactions represented by a Flory–Huggins interaction parameter or by the free energy penalty for deforming the thermoset network. Variations in the crosslink density near the interface within the thermoset are certain to affect the dynamics of interface formation as well as the equilibrium width.

EXPERIMENTAL

*d*PS (weight-average molecular weight = 6300, $R_g \approx 22$ Å, polydispersity = 1.04) was obtained from Polymer Sources (Canada). RSL 1462, a research-grade epoxy resin chemically identical to EPON 828 but having a high purity (low ionic content), was purchased from Shell Chemical Co. The aliphatic poly(ether triamine) curing agent T403 was obtained from Huntsman Chemical.[19] Both were used as received. The chemical structures of the resin and crosslinker monomers are

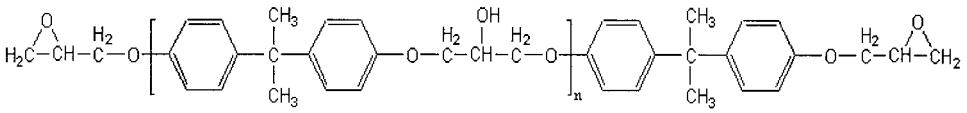

Shell EPON 828 Epoxy Resin

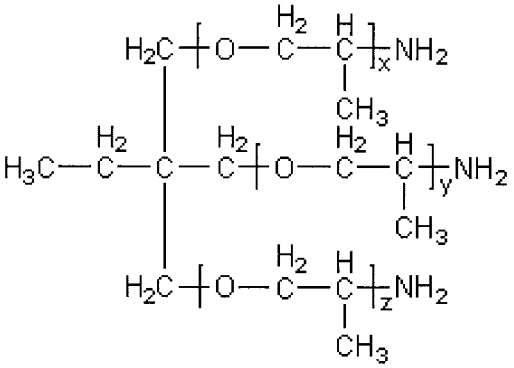

Huntsman T403 Curing Agent

Figure 1. Chemical structure of the diglycidyl ether of bisphenol A epoxy resin and the T403 poly(ether triamine) curing agent.

shown in Figure 1. The silicon wafer substrates were polished, 2-in.-diameter single crystals (111) obtained from Semiconductor Processing. Before deposition, the wafers were cleaned by being placed in a 60:40 mixture of H_2SO_4 and H_2O_2 (35%) at approximately 80 °C for at least 1 h, rinsed with deionized water, and then placed *in vacuo* at 45 °C for 24 h to remove the residual solvent. For the preparation of uniform thin epoxy films (250 ± 15 Å thick), the neat mixture was partially cured at 60 °C for 70 min and then dissolved in toluene. An aliquot was deposited onto a silicon wafer with a glass pipet and then spun off at 2300 rpm with a spin coater (Chemat Technology). Model bilayer films of *d*PS/epoxy (E*xx*) were prepared by the spin coating of the mixtures of the epoxy resin and aliphatic poly(ether triamine) curing agent from toluene solutions onto silicon wafers and the subsequent curing of the epoxy films. The label E*xx* represents an epoxy film with *xx* curing agent parts per 100 epoxy resin parts by weight. If these mixtures follow exclusively epoxide–amine addition reactions, about 46 amine parts per 100 epoxide parts is the stoichiometric mixture for complete cure. This is consistent with experimental measurements of the maximum glass-transition temperature and the minimum swelling ratio.[20] The epoxy films were cured at 80 °C for 1 h and then at 120 °C for 2 h in a vacuum oven, and this corresponds to a full cure condition.[17,18,20] Next, layers of *d*PS with thicknesses ranging from 45 to 600 Å were spin-cast from toluene solutions with polymer mass fractions between 0.1 and 3% onto the surfaces of the cured epoxy films. Six samples were prepared to examine the effects of the thickness of the *d*PS layer and the composition of the epoxy layer. All of the film thicknesses were measured with ellipsometry and confirmed with X-ray reflectivity (XR) or NR measurements. Equilibrium water contact angles, a measure of the surface energy and wettability of film surfaces, were determined for the epoxy films with a contact-angle goniometer (Rame–Hart) and found to be 42 ± 3, independent of the composition. The list of samples is shown in Table 1.

NR experiments on these bilayer films were conducted on the NG7 reflectometer (single wavelength, λ = 4.76 Å, $\Delta q/q$ = 0.03) at the National Institute of Standards and Technology and on the

Table 1. Bilayer Film Characteristics

Samples	Film Thickness (±3 Å) Bottom Layer (Epoxy)	Top Layer (*d*PS)	SLD of the Epoxy Layer (b/V × 10^{-6} Å^{-2})
E46-S45	262	45	1.127
E46-S320	232	320	1.127
E46-S600	228	602	1.127
E36-S320	246	338	1.190
E56-S320	285	322	1.064

POSY2 time-of-flight reflectometer (λ = 4–12 Å, $\Delta q/q$ = 0.04) at Argonne National Lab. The principles of the technique have been reviewed elsewhere.[21] Data analysis involves constructing a model neutron scattering length density (SLD) profile with a series of slabs of constant concentration, calculating the reflectivity from the stack of layers with the optical matrix method, and comparing the calculated curve to the experimental curve. The effects of roughness and finite interfacial width are included by each interface being divided into a number of small slabs to form a smooth gradient. Both in-plane roughness and a composition gradient lead to a gradient in the model one-dimensional SLD profile. Best fit parameters are determined by the minimization of the merit function, $\chi^2 = \Sigma[(R_m - R_c)/\sigma]^2/(N_p - N_d)$, with the Marquardt algorithm, where R_m is the measured reflectivity, R_c is the calculated reflectivity, σ is the standard deviation, N_p is the number of parameters, and N_d is the number of data points. NR experiments with films consisting of only a single epoxy layer were also performed to directly measure the SLD. These values were used to reduce the number of unknowns in fitting a model SLD profile to the NR data. The results are shown in Table 1. The reflectivity of the as-prepared samples was first measured, and then the samples were measured as a function of the annealing time. All of the samples were annealed at 123 ± 0.2 °C under high vacuum (~10^{-4} Torr), well above the glass-transition temperatures of all the PS and epoxy films used in this work.[22] On extended annealing of the samples at 123 °C, dewetting of the top *d*PS film was examined by atomic force microscopy (AFM; Digital Instruments NanoScope II in the tapping mode) and optical microscopy (Versamet-2 microscope in the reflection mode).

RESULTS AND DISCUSSION

The NR curves from E46-S45, consisting of a 45-Å layer of *d*PS on a 262-Å layer of epoxy, are shown for selected annealing times in Figure 2(a). The reflectivity for the as-prepared sample shows clear oscillations that are consistent with the values of the *d*PS film thickness (h_{dPS}) obtained from ellipsometry. There is only a slight difference between the as-prepared sample and the sample annealed for 7 min. However, at an annealing time of 20 min, the reflectivity is significantly lower for $q > \sim 0.07$ Å^{-1} relative to the as-prepared sample. The inset shows these data plotted as Rq^4 versus q to more clearly reveal the differences. As the annealing time increases beyond 20 min, the reflectivity for $q > 0.02$ Å^{-1} decreases dramatically because of a large increase in the surface roughness, which was confirmed by XR and AFM. In that case, the growth of surface undulations or spinodal dewetting was observed over the entire sample. These are explored in a subsequent article.[23] Because of the onset of spinodal dewetting, we were unable to measure the interfacial width of the E46-S45 sample for annealing times greater than 20 min

The solid curves through the data in Figure 2(a) are best fits with a multilayer SLD model with a hyperbolic tangent function introduced at the interfaces. The corresponding SLD profiles are shown in Figure 2(b). In the fitting, the interfacial roughness between epoxy and SiO_2 and the thickness of the SiO_2 layer were held constant at 4 and 15 Å,[9,17,21] respectively, where roughness (Δ) is defined as the root-mean-square (RMS) value of the deviation of the height relative to the average height of the surface. The RMS roughness is related to the interfacial width (λ) by $\Delta = \lambda/(2\pi)^{1/2}$. In the fitting procedure, both the roughness at the air surface and the interface width between *d*PS and epoxy were allowed to vary as fitting parameters for the annealed samples. These two factors affect the reflectivity curve in different ways, but the relative effects are also a function of the thicknesses of the two layers. These two effects could be clearly distinguished in the analysis of the NR data for the thicker *d*PS films (E46-S320 and E46-S600). For the E46-S45 sample, this distinction was aided by independent measurements of the surface roughness with AFM and XR.

The slight difference in reflectivity between the as-prepared sample and that after annealing for 7 min in Figure 2(a) corresponds to a small increase

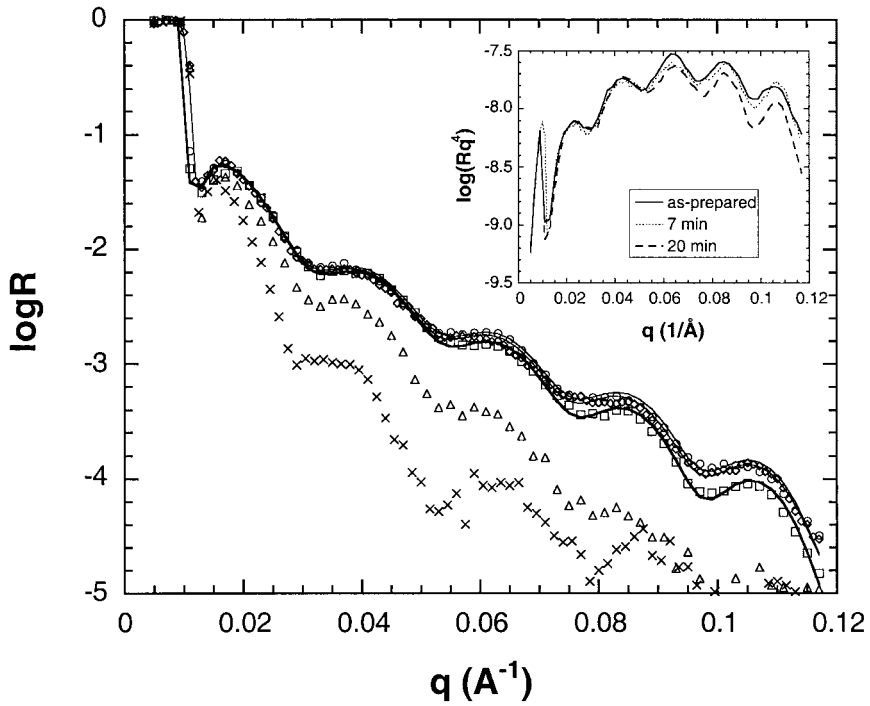

(a)

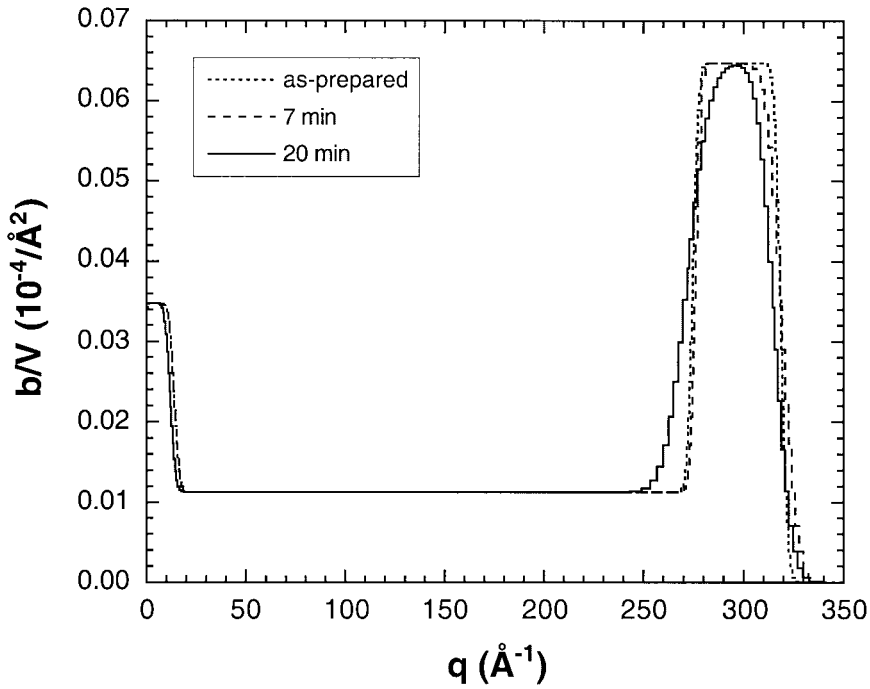

(b)

Figure 2. (a) NR from E46-S45 consisting of a 45-Å layer of *d*PS on a 262-Å layer of epoxy for selected annealing times at 123 ± 0.2 °C: (○) as-prepared, (◇) annealed 7 min, (□) annealed 20 min, (△) annealed 60 min, and (×) annealed 140 min. The curves through the data are best fit with a multilayer SLD model. The inset shows the reflectivity data plotted as Rq^4 versus q for annealing times up to 20 min. (b) Best fit SLD profiles corresponding to the curves through the data in part a for selected annealing times.

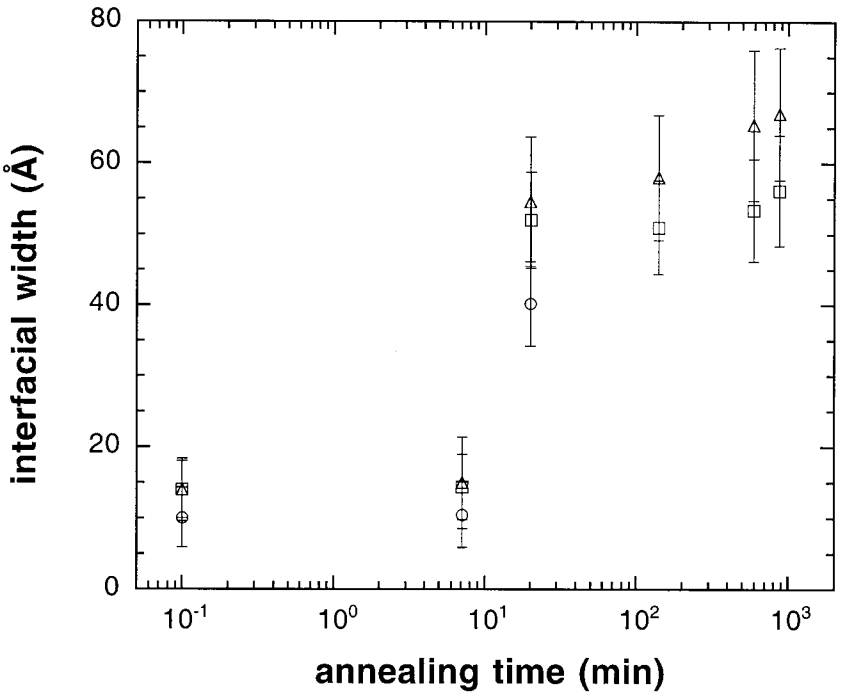

Figure 3. Interfacial width obtained from the NR data for three different $h_{d\mathrm{PS}}$ values (E46-S45, E46-S320, and E46-S600) as a function of the annealing time at 123 ± 0.2 °C: (○) E46-S45, (□) E46-S320, and (△) E46-S600.

in the surface roughness from 6 to 14 Å, whereas the interface width stays constant at about 10 Å. However, the change in the reflectivity observed between annealing times of 7 and 20 min is qualitatively different and is due largely to an increase in the interfacial width. The reflectivity data collected at 20 min of annealing indicate a surface roughness of approximately 16 Å and an interfacial width of approximately 42 Å. An independent measurement of the surface roughness at 20 min of annealing with AFM and XR indicated a value of approximately 15 Å.

The relatively short timescale for dewetting with the thin *d*PS film contrasts with that for the nucleation of holes for the thicker *d*PS films ($h > \sim 200$ Å). For example, we observed the nucleation of holes at an annealing time of approximately 20 h for the 330-Å PS film with a molecular weight of 6300 by optical microscopy. A similar observation for a 350-Å PS film (weight-average molecular weight = 4000) on a silicon substrate at 115 °C was reported by Karim et al.[24] At an annealing time of 25 h, they observed the nucleation of holes in the early stage of dewetting by AFM.

Figure 3 is a plot of the interfacial width (λ) versus the annealing time for E46-S45, E46-S320, and E46-S600 that shows the effects of $h_{d\mathrm{PS}}$ on the interfacial width at 123 °C. The main finding is that the effect is very weak. The interfacial width for all samples did not change up to 7 min of annealing but rather remained constant at about 12 Å. At an annealing time of 20 min, the interface width increased substantially for all film thicknesses. A difference in the interfacial width may exist for the E46-S45 relative to the other *d*PS layer thicknesses; however, these data are not conclusive. It is possible that the rate of diffusion of the *d*PS molecules into the epoxy film may be weakly affected by confinement effects for the case of the ultrathin *d*PS film. Such effects have been reported previously for film thicknesses of less than approximately $4R_g$.[25] The R_g value of our *d*PS is approximately 22 Å, so $h_{d\mathrm{PS}} = 45$ Å corresponds to $h = 2R_g$. The data may also suggest a weak dependence of the final equilibrium width on $h_{d\mathrm{PS}}$. This is similar to observations of the dependence of the equilibrium interfacial width on thickness reported for the PS/PMMA system.[9] Finally, we note that the magnitude of the interfacial width for this system is comparable to that reported for *d*PS/PMMA bilayer films. The reported values of the equilibrium interfacial width for the *d*PS/PMMA bilayer

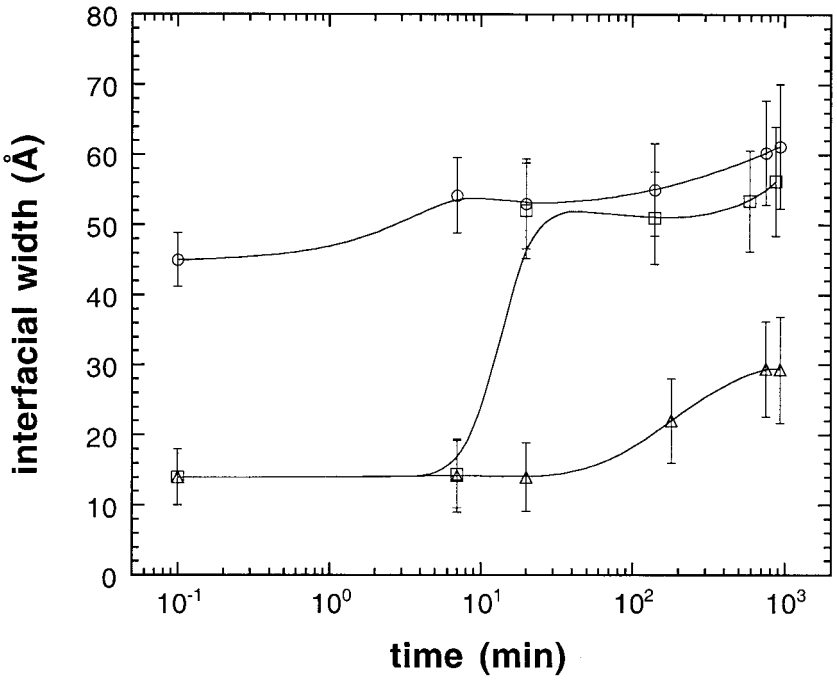

Figure 4. Interfacial width obtained from the NR data for three different resin/curing agent compositions (E36-S320, E46-S320, and E56-S320) as a function of the annealing time at 123 ± 0.2 °C: (○) E36-S320, (□) E46-S320, and (△) E56-S320.

films range from 40 to 70 Å, and this coincides with the range of interfacial widths of 50 ± 20 Å obtained here for the *d*PS/epoxy samples. The origin of the similar interfacial widths may indicate a similar χ parameter or may be simply fortuitous, as the interfacial width may result from very different phenomena in the two cases.

Figure 4 is a plot of the interfacial width versus the annealing time showing the effects of the resin/crosslinker composition on the interfacial width. Data are shown for E36-S320, E46-S320, and E56-S320 samples. For this series, the thickness of the *d*PS and epoxy layers were fixed at 330 ± 10 Å and 260 ± 30 Å, respectively. The behavior is markedly different for the three stoichiometries. For the E56-S320 sample (crosslinker excess), the interfacial width stays at a constant value of approximately 14 Å up to 20 min of annealing and then increases up to approximately 29 Å as the annealing time increases up to 930 min. In contrast, the interfacial width of the E46-S320 sample (stoichiometric composition) stays nearly constant at a value of approximately 14 Å up to 7 min of annealing, increases dramatically between 7 and 20 min of annealing, and then becomes nearly constant at approximately 56 Å for annealing times much greater than 20 min. For the E36-S320 sample (deficient in crosslinker), the interfacial width (~45 Å) obtained without annealing is much larger than the value (~14 Å) obtained for E46-S320 or E56-S320 without annealing. With further annealing up to 15 h, the interfacial width increases to approximately 60 Å, which is much larger than that of the E56-S320 sample. We confirmed that the surface roughness for all the samples fluctuated only slightly within a range of 4–10 Å as the annealing time increased up to approximately 15 h. The observed trend in the interfacial width with the epoxy composition can be understood if we consider the variation in the crosslink density near the interface observed previously. In previous work, several of us examined the crosslink density of single-layer epoxy films on silicon substrates by swelling the films with the good solvent nitrobenzene.[17] The principal observation was a significant segregation of the curing agent to the air surface, driven by the lower surface energy of the curing agent relative to the resin, which resulted in a lower crosslink density in the near-surface region. The effect was a strong function of the epoxy composition: E36 ≫ E46 > E56. This is consistent with the differences in the interfacial width as a function of the annealing time shown

in Figure 4. It is evident that the E36-S320 sample (crosslinker deficiency) shows a much larger interfacial width than that of the E56-S320 sample (crosslinker excess). Unreacted residual epoxide molecules are present in the near-surface region in E36 and contribute to the formation of an imperfect network structure in that region. These defects may allow more interdiffusion of PS molecules into the epoxy layer. For E56-S320, in contrast, the preferential segregation of the curing agent to the air surface may lead to a nearly stoichiometric composition because of the excess of curing agent in the bulk. This would then result in a more complete network structure in the near-surface region. Therefore, the more defect-free network structure in the surface region would explain the low degree of interpenetration for the E56-S320 bilayer film.

CONCLUSIONS

We have demonstrated that the interfacial width between PS and a highly crosslinked thermosetting epoxy is comparable to that of chemically different thermoplastic/thermoplastic interfaces and depends on the resin/curing agent composition of the epoxy layer. A small dependence on the film thickness of the *d*PS layer may exist as well. The resin/curing agent composition dependence of the interfacial width is likely due to the preferential segregation of the curing agent, which leads to the formation of defects in the network structure at the surface or near-surface region. These data for the PS/epoxy interfacial width are consistent with trends reported previously in the surface structure of thin epoxy films as a function of composition revealed by swelling. A slight suppression of interface broadening for thinner *d*PS films may indicate reduced mobility for film thicknesses smaller than approximately $4R_g$. Finally, we note that much more rapid dewetting was observed for the thinnest *d*PS film ($2R_g$).

The authors thank Richard Goyette for his assistance with the neutron reflectivity measurements at Argonne National Lab and Jessica Sorensen for the ellipsometry measurements. This work was supported by a New Mexico Tech grant (no. 11HX11049) and a Sandia National Laboratories grant (no. BG-7560). Sandia is a multiprogram laboratory operated by Sandia Corp., a Lockheed Martin company, for the U.S. Department of Energy under contract DE-AC04-94AL85000.

REFERENCES AND NOTES

1. Edward, E. Proc Phys Soc London 1965, 85, 613.
2. Helfand, E.; Tagami, Y. J Chem Phys 1972, 56, 3592.
3. Leibler, L. Macromolecules 1982, 15, 1283.
4. Binder, K. J Chem Phys 1983, 79, 6387.
5. Helfand, E.; Bhattacharjee, S. M.; Fredrickson, G. H. J Chem Phys 1989, 91, 7200.
6. Fernandez, M. L.; Higgins, J. S. Polymer 1988, 29, 1923.
7. Anastasiadis, S. H.; Russell, T. P.; Satija, S. K.; Majkrzak, C. F. J Chem Phys 1990, 92, 5677.
8. Schubert, D. W.; Stamm, M. Europhys Lett 1996, 35, 419.
9. Sferrazza, M.; Heppenstall-Butler, M.; Cubitt, R.; Bucknall, D.; Webster, J.; Jones, R. A. L. Phys Rev Lett 1998, 81, 5173.
10. Sferrazza, M.; Xiao, C.; Jones, R. A. L. Phys Rev Lett 1997, 78, 3693.
11. Merfeld, G. D.; Karim, A.; Majumdar, B.; Satija, S. K.; Raul, D. R. J Polym Sci Part B: Polym Phys 1998, 36, 3115.
12. Lin, E. K.; Kolb, R.; Satija, S. K.; Wu, W.-L. Macromolecules 1999, 32, 3753.
13. Bhala, M. J.; Freakley, P. K. Kautsch Gummi Kunstst 2001, 54, 394.
14. Wu, W.-L.; Wallace, W. E.; van Zanten, J. H.; Bauer, B. J.; Liu, D.-W. Polymer 1997, 38, 2583.
15. Kerle, T.; Yerushalmi-Rozen, R.; Klein, J. Macromolecules 1998, 31, 422.
16. Kerle, T.; Yerushalmi-Rozen, R.; Klein, J. Europhys Lett 1997, 38, 207.
17. Yim, H.; Kent, M.; McNamara, W. F.; Ivkov, R.; Satija, S.; Majewski, J. Macromolecules 1999, 32, 7932.
18. Yim, H.; Kent, M.; Jeon, H. S.; Smith, G. J Polym Sci Part B: Polym Phys 2002, 40, 1709.
19. Certain trade names and company products are identified to specify adequately the experimental procedure. The references to commercial equipment or materials do not imply recommendation or endorsement by the National Institute of Standards and Technology.
20. Morgan, R. J.; Kong, F.-M.; Walkup, C. M. Polymer 1984, 25, 375.
21. Russell, T. P. Mater Sci Rep 1990, 5, 171.
22. Kim, J. H.; Zang, J.; Zin, W. C. Langmuir 2000, 16, 4064.
23. Jeon, H. S.; Dixit, P. S.; Yim, H.; Kent, M. S. Manuscript in preparation.
24. Xie, R.; Karim, A.; Douglass, J. F.; Han C. C.; Weiss, R. A. Phys Rev Lett 1998, 81, 1251.
25. Muller-Buschbaum, P.; Gutmann, J. S.; Stamm, M. Macromolecules 2000, 33, 4886.